

Dynamic fracture model for acoustic emission

M. Minozzi^{1,2,3}, G. Caldarelli², L. Pietronero^{3,4}, and S. Zapperi^{4,a}

¹ Dipartimento di Fisica, Università di Roma 3, via della Vasca Navale 84, 00146 Roma, Italy

² INFN UdR Roma 1, Dipartimento di Fisica, Università “La Sapienza”, P.le A. Moro 2, 00185 Roma, Italy

³ CNR Istituto di Acustica “O. M. Corbino”, via del fosso del Cavaliere 100, 00133 Roma, Italy

⁴ INFN UdR Roma 1 and SMC, Dipartimento di Fisica, Università “La Sapienza”, P.le A. Moro 2, 00185 Roma, Italy

Received 22 May 2003 / Received in final form 19 September 2003

Published online 8 December 2003 – © EDP Sciences, Società Italiana di Fisica, Springer-Verlag 2003

Abstract. We study the acoustic emission produced by micro-cracks using a two-dimensional disordered lattice model of dynamic fracture, which allows to relate the acoustic response to the internal damage of the sample. We find that the distributions of acoustic energy bursts decays as a power law in agreement with experimental observations. The scaling exponents measured in the present dynamic model can be related to those obtained in the quasi-static random fuse model.

PACS. 62.65.+k Acoustical properties of solids – 46.50.+a Fracture mechanics, fatigue and cracks

1 Introduction

Crackling noise [1] is widely observed in systems as different as superconductors [2], magnets [3] or plastically deforming crystals [4]. A typical example is the acoustic emission (AE) recorded in a stressed material before failure. The noise is a consequence of micro-cracks forming and propagating in the material and should thus provide an indirect measure of the damage accumulated in the system. For this reason, AE is often used as a non-destructive tool in material testing and evaluation. Beside these practical applications, understanding the statistical properties of crackling noise has become a challenging theoretical problem. The distribution of crackle amplitudes follows a power law, suggesting an interpretation in terms of critical phenomena and scaling theories. This behavior has been observed in several materials such as wood [5], cellular glass [6], concrete [7] and paper [8] to name just a few.

The statistical properties of fracture in disordered media are captured qualitatively by lattice models, describing the medium as a discrete set of elastic bonds with randomly distributed failure thresholds [9–11]. After each failure the stress is redistributed in the lattice in a quasi-static approximation: i.e. the crack velocity is much slower than stress relaxation. Thus acoustic waves are not taken into account and the activity is monitored by the damage evolution or by the dissipated elastic energy. Numerical simulations indicate that micro-cracks propagate in avalanches giving rise to a heterogeneous response. The

avalanche distribution is typically described by power law distributions and the results are usually interpreted in the framework of phase transitions [12–16]. Despite the fact that critical phenomena are normally associated with a certain degree of universality (i.e. the scaling exponents should not depend on micro-structural details), there has been so far no quantitative agreement between models and experiments. A reason that could account for this discrepancy is the absence of acoustic waves in most models. It is then not obvious how to relate AE activity to internal avalanches. On the other hand, the interpretation of fracture as a critical phenomenon is still controversial [12–16].

Dynamic lattice models have been widely used in the past to analyze fracture processes [17–20], but although acoustic waves are explicitly included, the AE signal is usually not analyzed. Here we use a lattice model for dynamic fracture in a disordered medium, to obtain a direct correspondence between the recorded AE activity and the internal damage evolution. We find that the cumulative AE amplitudes are directly related — by a power law — to the cumulative damage. Next, we measure the distribution of the AE burst energies and find a power law with an exponent $\beta \simeq 1.7$ independent on the loading rate. This exponent can be related to the exponent describing failure avalanches in quasi-static models [12–16].

The paper is organized as follows: in Section 2 we define the model and report the results of our numerical simulations in Section 3. Finally, in Section 4 we provide a theoretical interpretation of the numerical data and present our conclusions.

^a e-mail: stefano.zapperi@roma1.infn.it

2 Model

We consider a scalar model of dynamic fractures where a two-dimensional lattice is loaded in mode III: the lattice lies in the (x, y) plane and deformation occurs along the z axis, so that the equations of elasticity become scalar. The equation of the motion for the anti-planar displacement u of a site with coordinate i, j is

$$\rho \ddot{u}_{i,j} = -K \sum_{(l,m)} (u_{i,j} - u_{l,m}) - \Gamma \dot{u}_{i,j}, \quad (1)$$

where the sum runs over the nearest neighbors (l, m) of site (i, j) , K is the elastic constant, ρ is the density and dissipation is simulated by a viscous damping with a constant Γ . Notice that a more realistic damping could be provided by a viscoelastic term (see for instance, in a different context, the model in Ref. [21]), but this would generate some complications in the numerical integration. In order to suppress some lattice effects, we use a 45 degree tilted square lattice. A constant strain rate is imposed to the model, by moving the boundary sites on two opposite boundaries at constant velocity V and $-V$, respectively. Periodic boundary conditions are imposed in the other direction. Disorder is simulated assigning randomly distributed failure threshold: a bond is removed (i.e. K is set to zero) when $\Delta u > f_c$, and f_c is uniformly distributed in $[0, 1]$. A model similar to ours was introduced and studied in the absence of disorder by Marder and Liu [18] and in the quasi-static limit ($V \rightarrow 0$, $\rho \rightarrow 0$, $\Gamma \rightarrow 0$) reduces to the random fuse model (RFM). In the RFM, a lattice of fuses with random thresholds break in response to an increasing voltage [10, 11]. Due to the scalar nature of our model there is a direct mapping between elastic and electric parameters [9]. The choice we made for the disorder distribution in the RFN corresponds to the limit of strong disorder, in which substantial damage is accumulated before the final fracture [10].

The equation of motion (Eq. (1)) is integrated numerically using a fifth order Runge-Kutta method. We work with a lattice of linear size $L = 80$ and chose the units of space and time so that $\rho = K = 1$. Each time a bond is stretched beyond its threshold the lattice constant is set to zero and an elastic wave is emitted. Due to the anti-plane constraint for the displacements, we only have transverse wave propagation with sound speed $c = \sqrt{K/\rho} = 1$ in our units. The damping constant is chosen to be $\Gamma = 0.1$ so that typical length traveled by a wave is a little smaller than the lattice size. For smaller values of Γ ringing effects and reflected waves do not allow to separate the single pulses and the lattice breaks at once. On the other hand, excessive damping leads to very small acoustic activity, which hinders a statistical analysis. Even if the damping constant is small reflected waves can induce boundary failure, due to the rigidity of the loaded edge. Thus we do not allow for bond failures in two boundary layers of length $l = 5$ close to the loaded edges. This corresponds to load through a soft contact, or a traction machine with an elastic constant of the order of the material constant.

The model is simulated for a variety of loading velocities all much lower than the sound speed $V \ll c$.

3 Simulation results

Measuring the displacements of every lattice site and calculating the forces for every time steps, we have obtained the stress-strain curve for four different value of the applied strain rate. In Figure 1 we show that the stress is a linear function of the strain up to the yield point, which precedes the total failure of the sample. The applied strain rate has little effect on the linear part of the curve, while it influences the curve after the peak. In particular, the drop in the stress is sharper for lower driving rates, because the time scale for internal stress relaxation is larger than the driving scale. Thus the dynamics approaches the quasistatic limit, where a sharp drop is expected [13]. On larger driving rates the two timescales are more interconnected and the breakdown is less sharp.

Monitoring the activity of some particular lattice sites we have direct access to the AE signal. These sites mimic the effect of transducers coupled to the material in a typical AE experiment. In a typical run, we record the displacements, velocities and accelerations of four sites in the boundary layer and two sites in the interior. Typically, AE distributions are recorded from a single site and averaged over ten realizations of the disorder. We have tested that the statistical properties of the signal do not vary for different boundary sites, while there is a clear difference between boundary and inner sites. In the following, we concentrate on sites in the boundary layer, in order to avoid excessive fluctuations due to failures occurring on neighboring bonds in the inner region.

An example of the typical signals recorded with our model are reported in Figure 2. A large acoustic activity is visible in the upper panel where we show the local acceleration a of a boundary site as a function of time. We can also monitor the velocity signal which is simply related to the acceleration and display the same features. In the present model, it will be convenient to use the acceleration as a AE monitoring tool, since the velocity has a bias induced by the external loading: even in the absence of cracking the lattice has a non-vanishing velocity. We define the associated cumulative energy as

$$E(t) \equiv \int_0^t dt' a^2(t'). \quad (2)$$

The behavior of the cumulative acoustic energy $E(t)$ is typically monitored in AE experiments. In some cases, $E(t)$ is found to increase as a power law [5], or exponentially in other cases [8]. In general one expects a marked peak close to failure, as we also observe in Figure 2, obtained for $V = 10^{-3}$. The curve follows quite well a cubic law, $E \sim t^3$, apart from sample fluctuations, which become larger close to the final breakdown. Similar fluctuations are observed in experiments and have been the object of an intense theoretical analysis [22].

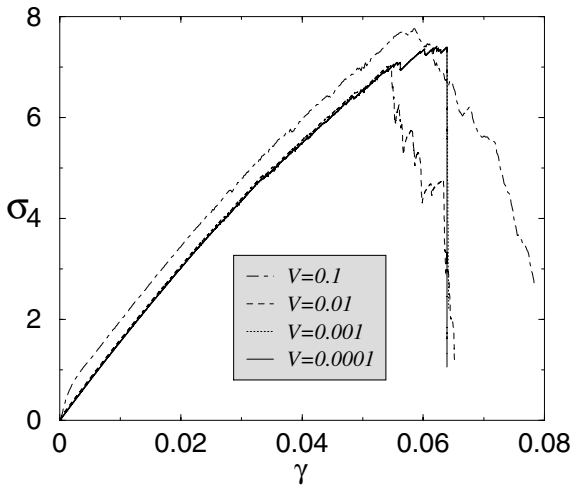


Fig. 1. The stress-strain curve for different applied strain rates.

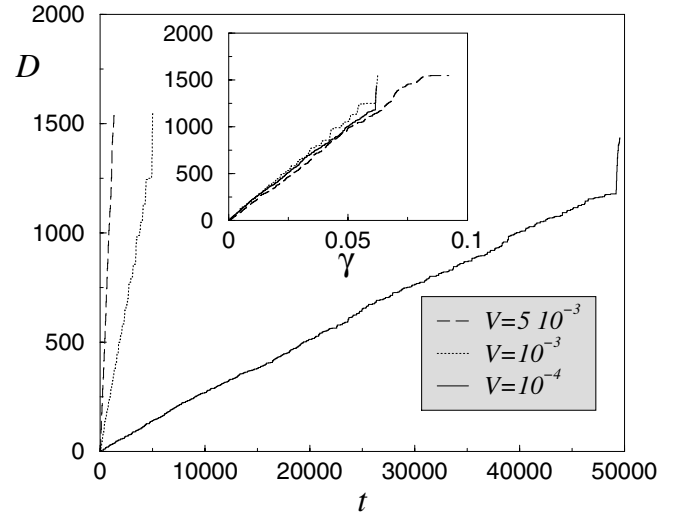


Fig. 3. The damage D evolution is displayed as a function of time for different loading rates. The curves collapse onto each other when plotted with respect to strain $\gamma \equiv Vt/L$.

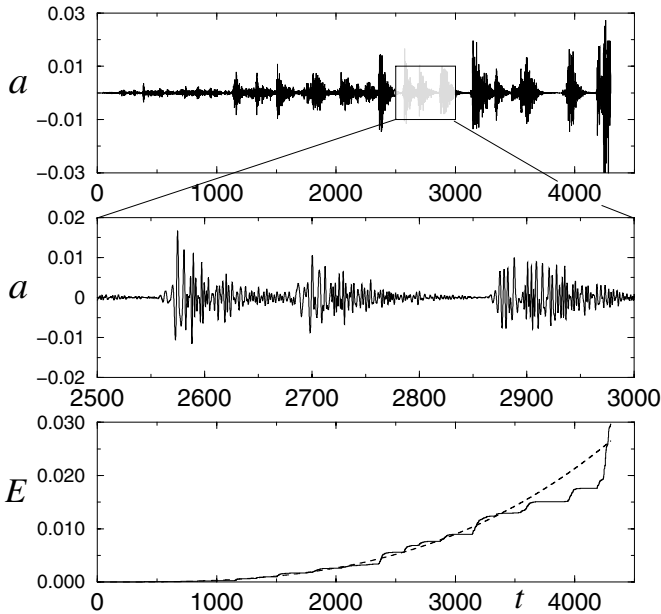


Fig. 2. A typical signal measured in the model. The upper panel shows the velocity acceleration of a site close to the boundary. In the middle panel we show a magnification of a portion of the signal. In the lower panel is reported the cumulative energy, $E(t) \equiv \int_0^t dt' a^2(t')$, as a function of time for a single realization of disorder. The dashed line follows t^3 .

A central problem in AE measurements is to correlate the recorded acoustic activity with the internal damage state. In this way, AE can be used as a tool for damage evaluation. In our model, we have a direct access to the internal damage D that can be defined as the total number of failed bonds. We find that D increases linearly with time (see Fig. 3) apart from a rapid increase very close to failure. Rescaling the curves with the loading rate one

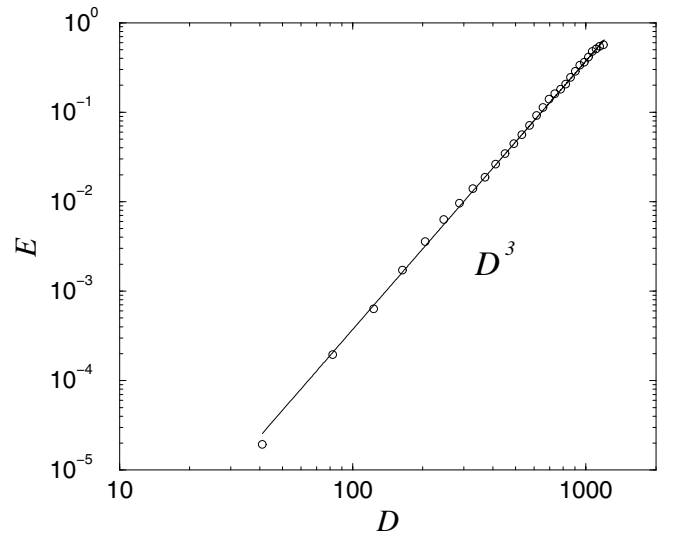


Fig. 4. The average cumulative energy plotted as a function of damage. The line represents a D^3 law which fits well the curve.

sees that D is in fact a linear function of the applied strain $\gamma \equiv (Vt)/L$ (see the inset of Fig. 3) [25].

These observations thus lead to a direct scaling relation between internal damage and released acoustic energy: Figure 4 shows that E scales as D^3 . This result can be explained assuming that the cumulative acoustic energy E is proportional to the total released elastic energy $E_{el} \sim KD\gamma^2 \sim D^3$.

As we discussed in the introduction, a common feature of crackling noise experiments is the power law distribution of the AE bursts. In Figure 5 we report the distribution of energy bursts measured in our model for the acceleration signal, defining $\epsilon \equiv a^2$. We show the results for two values of the driving velocity and in both cases

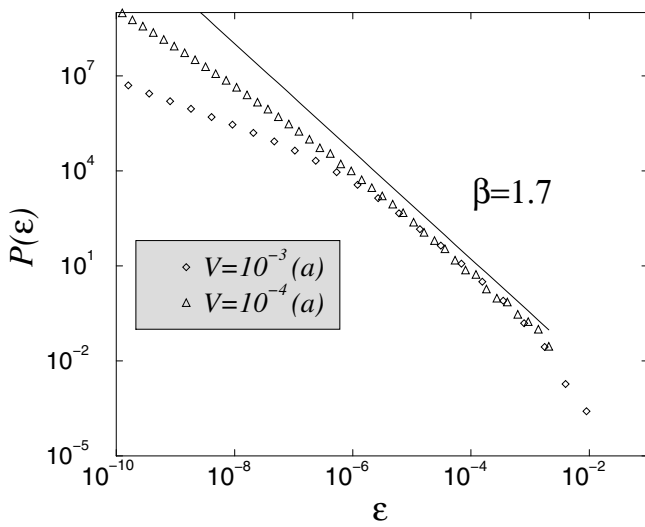


Fig. 5. The distribution of acoustic burst energies for different driving rates. The line is a power law with exponent $\beta = 1.7$.

the distribution decays as power law with an exponent $\beta = 1.7 \pm 0.1$, independent on the loading rate, which only affects the low part of the distribution. This behavior could be expected since for a higher driving rate some pulses overlap, leading to a depletion of the number of small avalanches as observed in Figure 5. The same results are found in the case of the velocity signal. Experimental results report an exponent value in the same range, even if it differs a little from one material to another: for wood the exponent is $\beta = 1.51 \pm 0.05$, for fiberglass $\beta = 2.0 \pm 0.01$ [5], $\beta = 1.30 \pm 0.1$ for paper [8], $\beta = 1.5 \pm 0.1$ for experiments on cellular glass [6].

4 Discussion and outlook

A large amount of theoretical activity has been devoted in the past to understand the origin of power law distributions of AE amplitudes widely observed in material fracture. Most of the analysis was devoted to quasi-static models, such as the the RFM, where fracture was shown to occur in damage burst, whose size ΔD is distributed as $P(\Delta D) \sim (\Delta D)^{-\tau}$ with $\tau \simeq 2.5$ [12,13]. This value is in perfect agreement with the result $\tau = 5/2$ obtained exactly [23] for the exponent of the avalanche distribution of the fiber bundle model (FBM) [24], where N fibers with random failure threshold are loaded in parallel. It was thus conjectured that the long-range stress transfer present in the RFM was equivalent to the infinite range load redistribution of the FBM, placing the two models into the same universality class [12,13]. A similar exponent was found in a vectorial fracture model, so that this class could be even broader [13]. Comparing this result with AE experiments is problematic since quasi-static models do not account for wave propagation.

In quasistatic models, it is possible to define unambiguously a damage burst ΔD , counting the number of

failures due to a small increase of the external load. This is not the case in a dynamic model, where there is no time scale separation between driving and fracture. Nevertheless, also in this case the failure process is clustered both in space and time, with quiescent intervals followed by rapid bursts of activity. An indirect measure of these process can be obtained by the distribution of pulse energies in the acoustic activity, reported in Figure 5. Using the scaling relation between released acoustic energy and damage discussed above, we can relate the energy exponent β to the damage exponent τ , which can be directly measured only in quasistatic models. From $E \sim D^3$ and $D \sim t$, we expect $\epsilon \sim D^2$. Substituting this expression in the equation for the probabilities, assuming $\Delta D \sim D$ (i.e. the typical avalanche size grows as the damage grows) $P(\epsilon)d\epsilon = P(\Delta D)d(\Delta D)$, we obtain $\tau = 1 + 2(\beta - 1) = 2.4$, which is very close to $\tau = 5/2$ measured in the RFM. Thus we conjecture that the acoustic energy exponent measured in our dynamic model is directly related with the damage exponent measured in the corresponding quasi-static model [26].

In conclusions, we have introduced a lattice model of dynamic fracture which can be used to model AE experiments. The model allows to clarify important issues in the interpretation of the experiments, namely the relation between internal damage and released acoustic energy. In particular, we derive direct relations between the scaling behavior of failure avalanches and acoustic bursts. It would be interesting to generalize this analysis to more realistic situations, exploring the role of dimensionality, load conditions and lattice anisotropy. However, in comparing the simulated signal with experiments, we should be careful about the definition of the events in the time series, since the amplifier and the AE sensors could bias the recorded waveform, introducing a systematic error in the data.

This work has been supported by the INFM center SMC.

References

1. J. Sethna, K.A. Dahmen, C.R. Myers, *Nature* **410**, 242 (2001)
2. S. Field, J. Witt, F. Nori, X. Ling, *Phys. Rev. Lett.* **74**, 1206 (1995)
3. G. Durin, S. Zapperi, *Phys. Rev. Lett.* **84**, 4705 (2000)
4. M.C. Miguel, A. Vespignani, S. Zapperi, J. Weiss, J.R. Grasso, *Nature* **410**, 667 (2001)
5. A. Garcimartín, A. Guarino, L. Bellon, S. Ciliberto, *Phys. Rev. Lett.* **79**, 3202 (1997); A. Guarino, A. Garcimartín, S. Ciliberto, *Eur. Phys. J. B* **6**, 13 (1998)
6. C. Maes, A. Van Moffaert, H. Frederix, H. Strauven, *Phys. Rev. B* **57**, 4987 (1998)
7. A. Petri, G. Paparo, A. Vespignani, A. Alippi, M. Costantini, *Phys. Rev. Lett.* **73**, 3423 (1994)
8. L.I. Salminen, A.I. Tolvanen, M.J. Alava, *Phys. Rev. Lett.* **89**, 185503 (2002)
9. *Statistical Models for the Fracture of Disordered Media*, edited by H.J. Herrmann, S. Roux (North Holland, Amsterdam, 1990)

10. L. de Arcangelis, S. Redner, H.J. Herrmann, *J. Phys. Lett. Paris* **46**, L585 (1985)
11. P.M. Duxbury, P.D. Beale, P.L. Leath, *Phys. Rev. Lett.* **57**, 1052 (1986)
12. A. Hansen, P.C. Hemmer, *Phys. Lett. A* **184**, 394 (1994)
13. S. Zapperi, P. Ray, H.E. Stanley, A. Vespignani, *Phys. Rev. Lett.* **78**, 1408 (1997); *Phys. Rev. E* **59**, 5049 (1999)
14. S. Zapperi, A. Vespignani, H.E. Stanley, *Nature (London)* **388**, 658 (1997)
15. G. Caldarelli, F.D. Di Tolla, A. Petri, *Phys. Rev. Lett.* **77**, 2503 (1996)
16. V.I. Räsänen, M.J. Alava, R.M. Nieminen, *Phys. Rev. B* **58**, 14288 (1998)
17. See J. Fineberg, M. Marder, *Phys. Rep.* **313**, 1 (1999), for a review on dynamic fracture
18. M. Marder, X. Liu, *Phys. Rev. Lett.* **71**, 2417 (1993)
19. T.T. Rautiainen, M.J. Alava, K. Kaski, *Phys. Rev. E* **51**, R2727 (1994); *ibid.* **56**, 6443 (1997)
20. T. Martín, P. Español, M.A. Rubio, I. Zúñiga, *Phys. Rev. E* **61**, 6120 (2000)
21. R. Ahluwalia, G. Ananthakrishna, *Phys. Rev. Lett.* **86**, 4076 (2001)
22. Y. Huang, H. Saleur, C. Sammis, D. Sornette, *Europhys. Lett.* **41**, 43 (1998); D. Sornette, J.V. Andersen, *Eur. Phys. J. B* **1**, 353 (1998)
23. P.C. Hemmer, A. Hansen, *J. Appl. Mech.* **59**, 909 (1992); M. Kloster, A. Hansen, P.C. Hemmer, *Phys. Rev. E* **56**, 2615 (1997)
24. H.A. Daniels, *Proc. Roy. Soc. London A* **183**, 405 (1945); S.L. Phoenix, H.M. Taylor, *Adv. Appl. Prob.* **5**, 200 (1973)
25. In quasistatic models, the damage displays a singular derivative when plotted against stress. This could also be found in our model if we invert the stress-strain curve. The peak in the curve translates into a singular derivative in the inverse curve
26. The distribution of the “elastic” energy released in each avalanche was recently measured in the quasi-static FBM and found to decay as power law with exponent $\beta \simeq 1.8$ [8], in agreement with our results